

# **Determining an Exoplanet's Rotational Period Through Spectral Analysis Methodologies**

Weihong Cen

## Abstract

The rotational period of an exoplanet is needed to understand its formation. To obtain the rotational period, previous research performed time-series analysis on a single-point light source. Simulated Earth images were created from more than 5 years of DSCOVR Earth images, and the data for reflected visible and infrared light were extracted from Earth's obliquity, topography, atmosphere, vegetation, cloud patterns, and rotational period. The simulation is studied as an exoplanet to find the minimum sample collection rate required to determine the rotational period. Due to Earth's topography, the irradiance is different depending on the region photographed. By applying Fourier transform to the data, we can find the frequency in which a particular region reappears during the time-series. The purpose of this research is to find methods that could derive an exoplanet's rotational period with a longer sampling interval. The research takes into consideration the long exposure time required to image exoplanets. Because the correct rotational period would be less noticeable as the sampling interval increases, this research experiments with different methodologies to address the imaging limitations.

## 1. Introduction

Directly imaging exoplanets could provide more information about their surface composition using different wavelengths of radiation. However, current telescopes require long exposure times to directly image bright exoplanets that orbit at a great distance from their host star, with the average known planetary radius being 1.5 Jupiter radii. Such a limitation means that an imaged planet's rotational period might be shorter than the sampling interval, which makes determining its rotational period difficult.

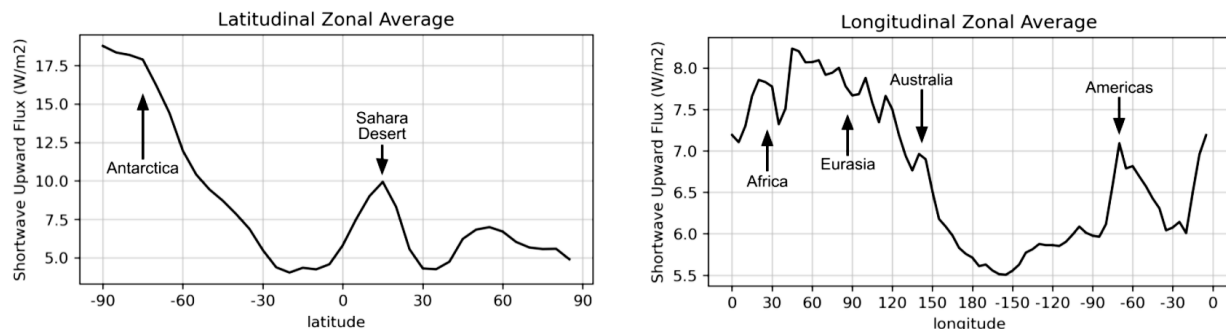
The purpose of this experiment is to reduce the number of image samples per day required to determine the rotational period. Simulated planets are used to provide outputs needed for direct imaging. The planetary parameters being Earth-like, land, aqua surfaces, and rotational periods of 24 and 72 hours. Here, the outputs for shortwave upward flux (FUS) and longwave upward flux (FUL) are studied.

Fourier transform is used as the main method to understand the frequency of a time-series. Different methods are then used to analyze the Fourier power spectra of the simulated planet's time-series.

## 2. Fourier Analysis

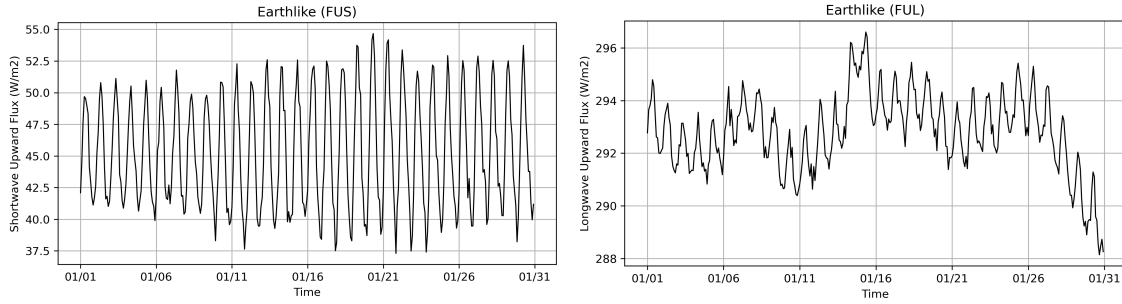
Fourier transform has versatile applications, from deconstructing audio to its base frequencies to processing images. In this research, we used Fourier transform on astronomical data.

Irradiance differs with different materials: land, cloud, and ice reflect more radiation than water. As shown in Figure 1, Areas with more landmass display a higher shortwave upward flux, while less visible light is reflected by the ocean (see Figure 18 in the [Appendix](#)).



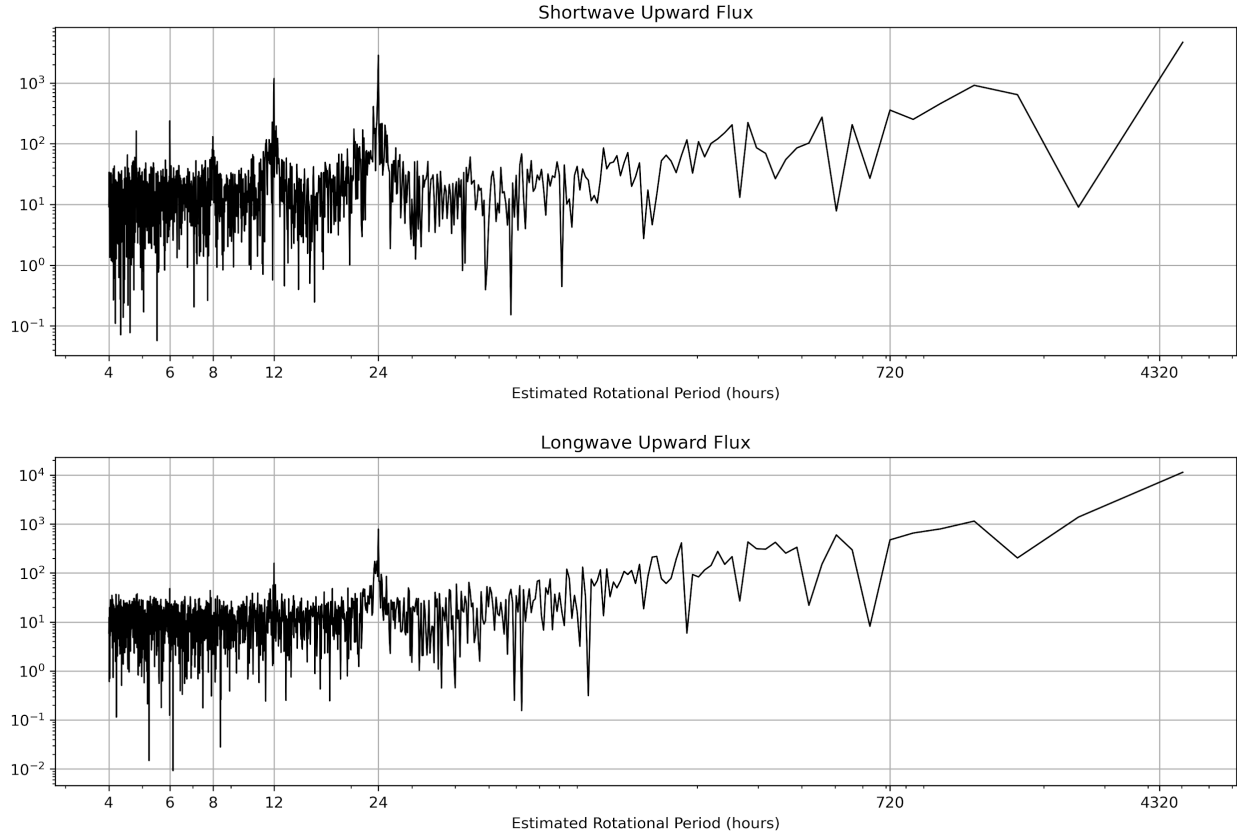
**Figure 1.** Zonal average of shortwave upward flux in January. The left panel shows the average at different latitudes and the right panel shows the average at different longitudes.

As a planet rotates, the time-series of its reflected radiation would have a sinusoidal trend. In Figure 2, the time-series for both visible and infrared radiation oscillates 30 times, which corresponds to the number of days in the dataset: from the start of January 1st to the start of January 31st. However, counting the oscillations is time-consuming and would not be useful if the observational interval is longer than the rotational period. A Fourier power spectrum then is better suited to obtaining the rotational period of an exoplanet.



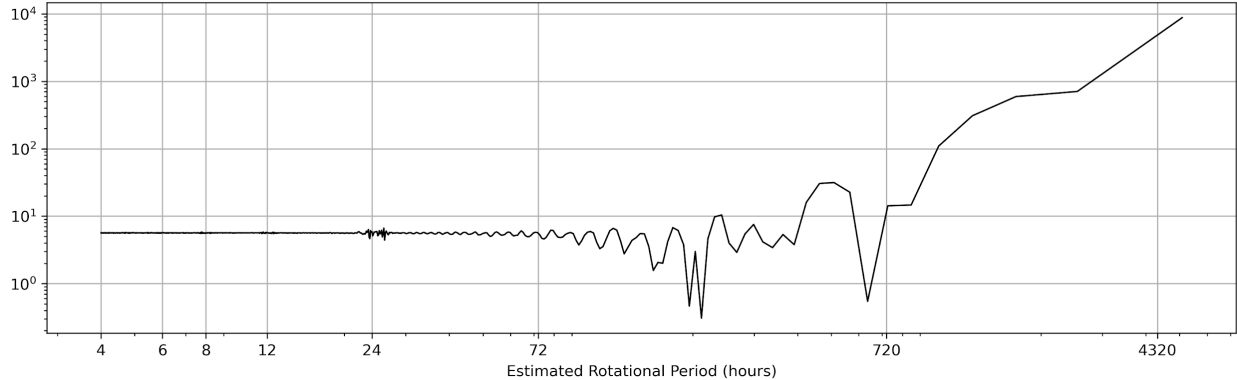
**Figure 2.** time-series of shortwave upward flux (left panel) and longwave upward flux (right panel) of an Earth-like planet.

Fourier transform could be applied to the sinusoid to obtain its frequency, which in this case is the rotational period. Figure 3 demonstrates that it is easier to discern the rotational period of shortwave upward flux compared to the longwave upward flux. Additionally, even with a sampling interval of 12 hours, it is still possible to discern the correct rotational period (see Figure 11 in the [Appendix](#)).



**Figure 3.** Fourier series power spectra of visible light (top panel) and infrared light (bottom panel)

However, a drawback to this method is that it utilizes the difference in irradiance over different topographies. This would make it more difficult to pick up the rotational period of exoplanets with a uniform type of topography. Here, Fourier transform is performed on land planets and aqua planets to demonstrate the difference (Figure 4). The Fourier power spectrum for the land planet only shows a small fluctuation at the frequency of 24 hours, and the Fourier power spectrum for the aqua planet shows a less significant peak at 24 hours than the Earth-like planet. One reason that the aqua planet still shows a peak compared to the land planet would most likely be because of its cloud formation during the simulation. As different areas generally have different concentrations of clouds, the irradiance difference would show a sinusoidal trend.



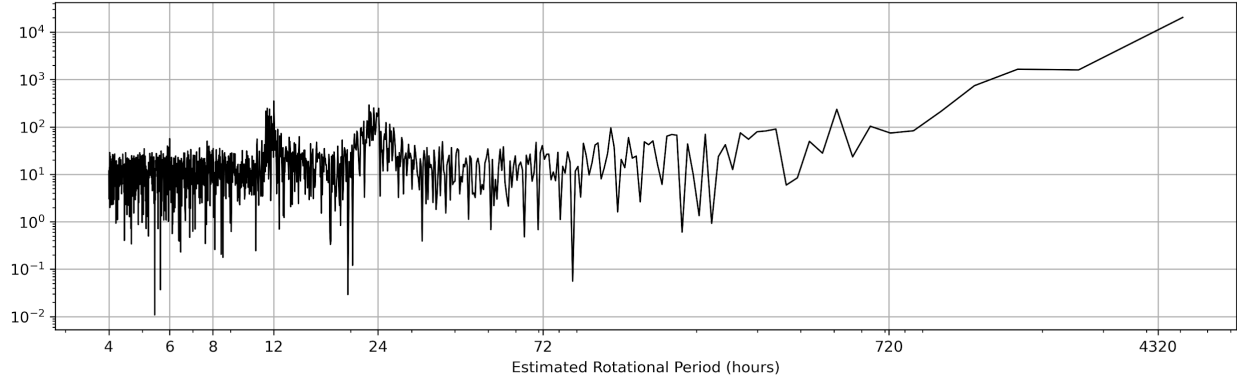


**Figure 4.** Fourier power spectra of shortwave upward flux for the land planet (top panel) and the aqua planet (bottom panel) with a sampling interval of 2 hours.

### 3. Probability of Detecting Diurnal Cycle

I averaged each section of the dataset to replicate different exposure times. For example, the original dataset spans 105 days and has a sampling interval of 2 hours; to simulate a dataset with a sampling interval of 18 hours, I would replace every 9 data points with their average.

Using the dataset, Fast Fourier transform is applied to random 30-day segments. With a long sampling interval, the Fourier power spectrum would exhibit a logarithmic behavior (Figure 5). This would make it more difficult to find the correct peak, so I recorded the peak of the graph at different starting points, which helps me better visualize the position of peaks. As shown in Figure 5, the probability of detecting diurnal cycle changes according to the starting point of the Fourier power spectrum, with jumps at 10 and 20 indicating peaks at frequencies of 72 hours and 36 hours.

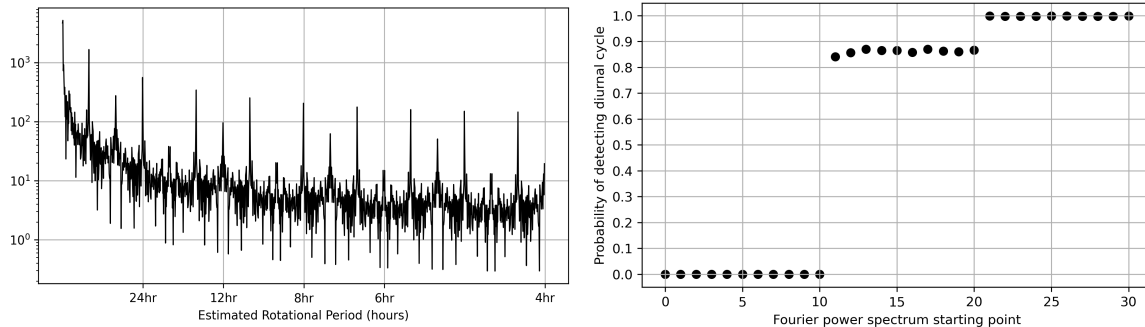


**Figure 5.** Fourier power spectrum of a dataset with an 18-hour sampling interval (left panel) and the probability of detecting the diurnal cycle from each Fourier power spectrum starting point (right panel).

To test how different sampling intervals could affect the probability of detecting the diurnal cycle, I averaged the probability at different starting points for each sampling interval (Figure 5). Table 1 shows that there is a relatively high chance of detecting the correct rotational period if the number of samples per day is greater than 2.

One outlier is the land planet with a 24-hour rotational period, which has a much higher probability of detecting the diurnal cycle with a sampling interval of 24 hours instead of 2 hours. However, this may be the result of the shortwave upward flux resembling a step function.

**Table 1**

Earth-like Planet with a 24-hour Rotational Period			Earth-like Planet with a 72-hour Rotational Period		
Sampling Interval (hr)	Number of Samples per Day	Probability of Detecting Diurnal Cycle	Sampling Interval (hr)	Number of Samples per Day	Probability of Detecting Diurnal Cycle
2	12	1.000	6	12	0.671
4	6	1.000	12	6	0.700
6	4	1.000	18	4	0.701
8	3	0.996	24	3	0.727
10	2.4	0.993	30	2.4	0.596
12	2	0.993	36	2	0.653
14	1.71	0.606	42	1.71	0.282
16	1.5	0.500	48	1.5	0.371
18	1.33	0.620	54	1.33	0.307
20	1.2	0.558	60	1.2	0.313
22	1.09	0.112	66	1.09	0.294
24	1	0.137	72	1	0.219

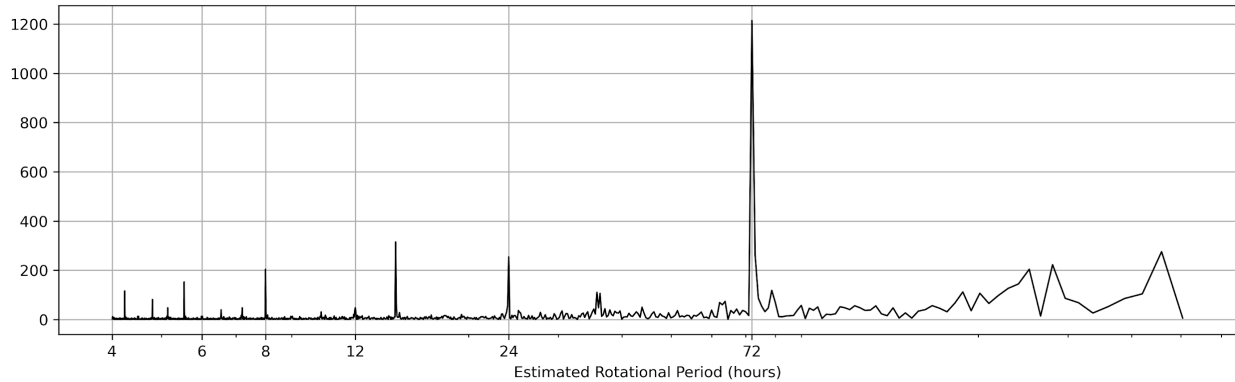
  

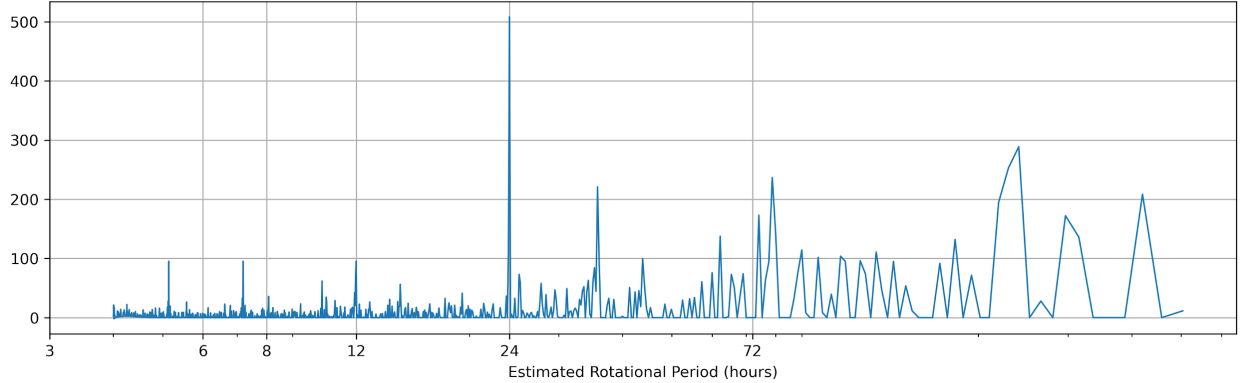
Land Planet with a 24-hour Rotational Period			Aqua Planet with a 24-hour Rotational Period		
Sampling Interval (hr)	Number of Samples per Day	Probability of Detecting Diurnal Cycle	Sampling Interval (hr)	Number of Samples per Day	Probability of Detecting Diurnal Cycle
2	12	0.075	2	12	0.669
4	6	0.070	4	6	0.724
6	4	0.068	6	4	0.739
8	3	0.066	8	3	0.653
10	2.4	0.063	10	2.4	0.608
12	2	0.053	12	2	0.639
14	1.171	0.048	14	1.71	0.237
16	1.5	0.034	16	1.5	0.244
18	1.333	0.028	18	1.33	0.124
20	1.2	0.022	20	1.2	0.065
22	1.091	0.001	22	1.09	0.027
24	1	0.355	24	1	0.267

#### 4. Detrending & Complex Numbers

Detrending could help with finding a peak without removing the peak at the start of a Fourier power spectrum that is a result of Fourier transform. As using Fourier transform usually results in a spike at frequency = 0, the usual method is to offset the graph or remove the DC component. However, with a long sampling interval, it becomes difficult to filter the spike (Figure 12).

First, I used a quadratic detrend as an experiment on the Fourier power spectrum. When applied to a Fourier power spectrum of the Earth-like planet with a sampling interval of 18 hours, the new peak becomes 24 hours while the original peak was at 72 hours (Figure 6). A similar result could be seen with a sampling interval of 14 hours (see Figure 14 in the Appendix)

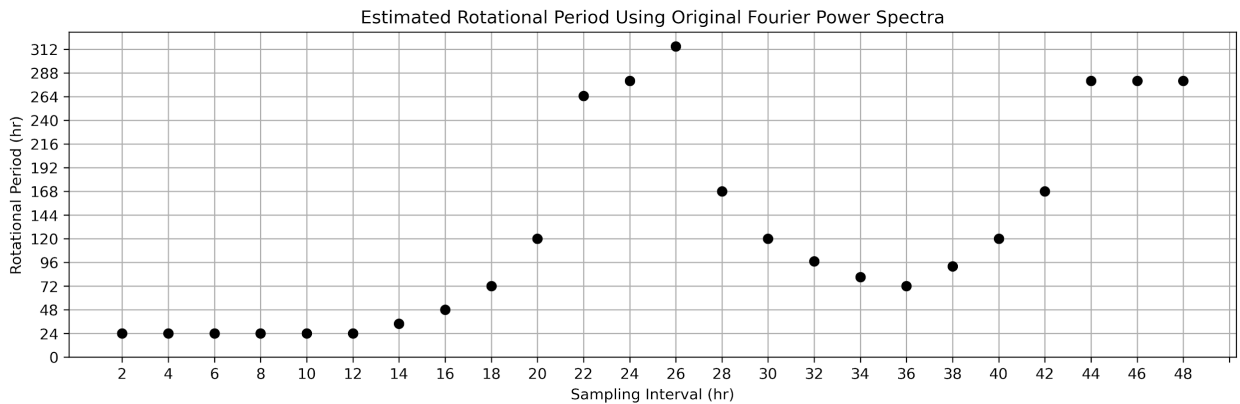




**Figure 6.** Fourier power spectrum of the Earth-like planet with a sampling interval of 18 hours (top panel), and its detrended graph using a 50th order polynomial (bottom panel).

A possible reason for this might be because the Fourier transform outputs an array of complex numbers, as it involves wrapping the graph around a circle to find the center of mass. Pyplot would discard the imaginary component when graphing as shown in the top panel of Figure 6, resulting in a peak at 72 hours, while the imaginary component has a valley at 72 hours as well (see Figure 13 in the Appendix). So, by taking the sum of both components if the imaginary component is used as a real number, the rotational period at 24 hours would have a greater magnitude.

Although taking the sum of the two components does not seem to affect the already-correct predictions, the better way to consider the complex number is to use the Pythagorean theorem and obtain the hypotenuse on a complex number plane, which yields similar results to only taking the Fourier power spectrum of the real number component.



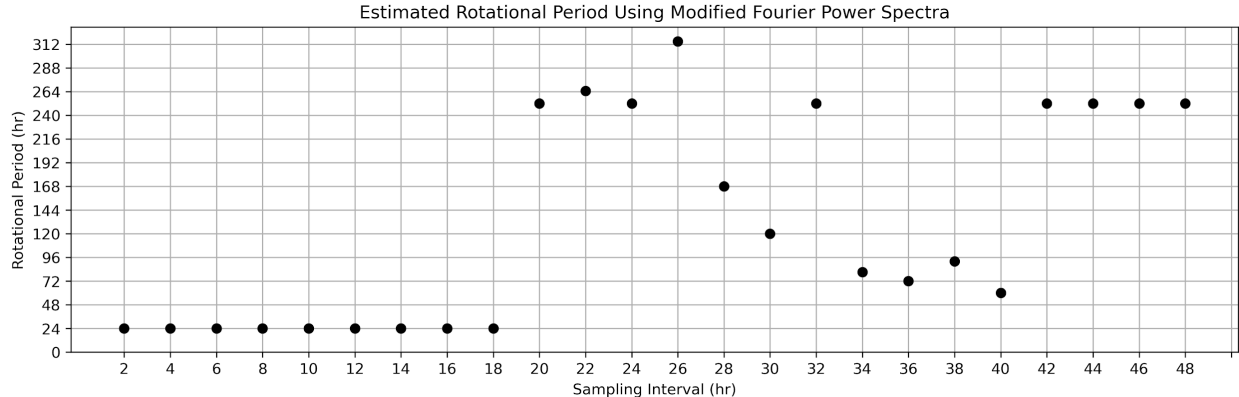


**Figure 7.** The probability of detecting the diurnal cycle from each Fourier power spectrum's starting point for the Fourier power spectrum of an Earth-like planet with a 2-hour sampling interval. The top panel shows the power spectrum with a discarded imaginary number, while the bottom panel takes the sum of the real and imaginary components.

Because a Fourier power spectrum resembles an exponential graph on a linear scale but a logarithmic graph on a log scale (Figure 12), I also experimented with using quadratic detrend on the natural log of the Fourier power spectra. However, the result is less satisfactory as the detrended peak tends to vary between 24, 12, 8, 6, and 2 hours.

Another attempt to detrend the data is to remove the DC component. To do that, the data must fit on  $x = 0$ . Two methods were attempted.

The first method is to align the average of the graph to the x-axis before applying Fourier transform. However, monthly irradiance differs from the planet's distance from the star, so the DC component is not reduced by much.

The second method is more effective than the first: by taking the difference between each data point. This method captures the 1st discrete difference along the dataset. The resulting graph shows a noticeable reduction in the DC component (see Figure 16 in the Appendix).

One downside to the second method is that it is less effective for data with long sampling intervals, which is the opposite of this research's intended purpose.

## 5. Compiling Different Sampling Intervals

When the number of samples per day is less than 2, the probability of detecting the diurnal cycle decreases drastically (Table 1). However, a peak at the correct rotational period would still be visible in the Fourier power spectrum. This method could help visualize the peak through graphs with different sampling intervals.

First, I recorded the peak of the Fourier power spectra from different starting points to better visualize the position of peaks. In Figure 8 every point represents the peak of the Fourier power spectrum after a specific part of the spectrum. Then, I overlapped graphs with different sampling intervals together, with each graph opaque.

As seen in Figure 8, the majority of the sampling intervals exhibits a Fourier power spectrum peak at 24 hours. When graphed individually, the peaks are evenly spaced. However, a collection of graphs would show a concentration of peaks at a rotational period of 24 hours.

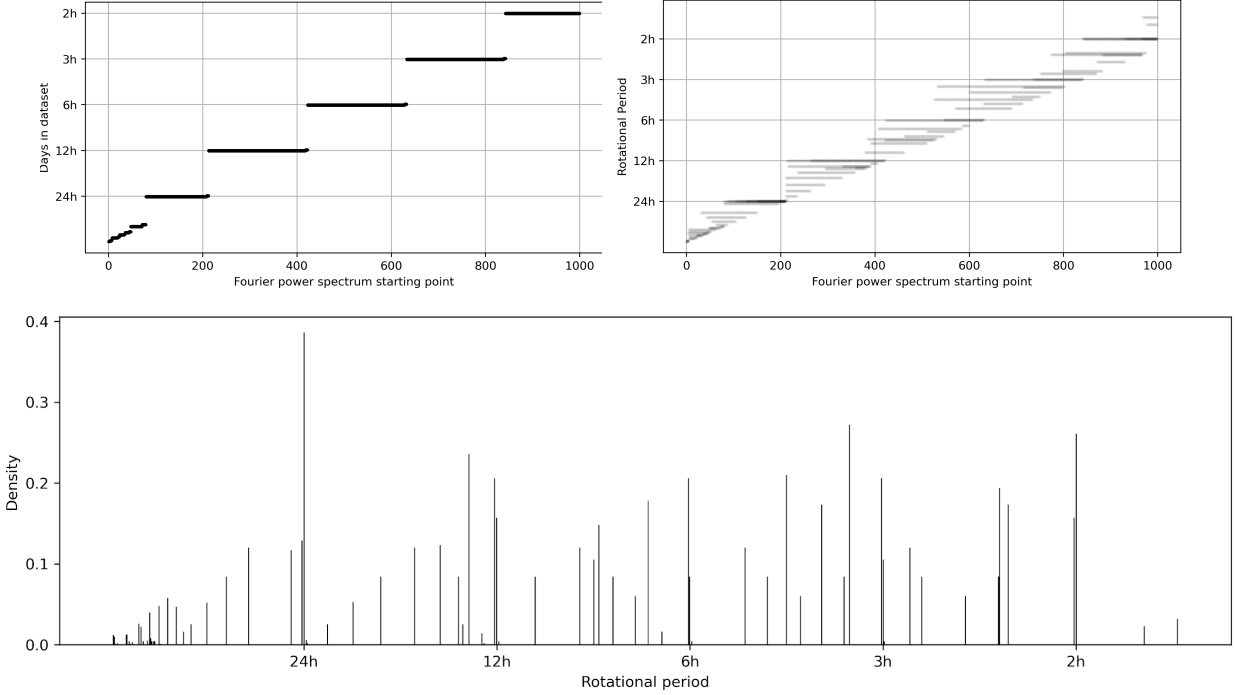


**Figure 8.** Graph for a sampling interval of 24 hours with the most likely rotational periods at different Fourier power spectrum starting points (top-left panel), and the compiled graphs of sampling intervals from 24 hours to 36 hours (top-right panel). The figure to the right shows a concentration of rotational periods at 24 hours for an Earth-like planet with a 24-hour rotational period. The bottom figure helps visualize the density of the data points at each rotational period.

Unlike the method used to record Table 1, this method requires the time-series from many different observational intervals. While the main drawback is the amount of imaging required concurrently, it could show the correct rotational period more reliably without the need to increase the daily number of samples, even when the sampling interval is more than twice the length of the rotational period (see Figure 17 in the Appendix).

## 6. Longwave Upward Flux and Vegetation Correlation

When comparing the time-series of shortwave upward flux with longwave upward flux, the aqua planet and terrestrial planet with no bodies of water show a parallel between reflected wavelengths. However, an Earth-like planet does not exhibit this similarity (Figure 9).

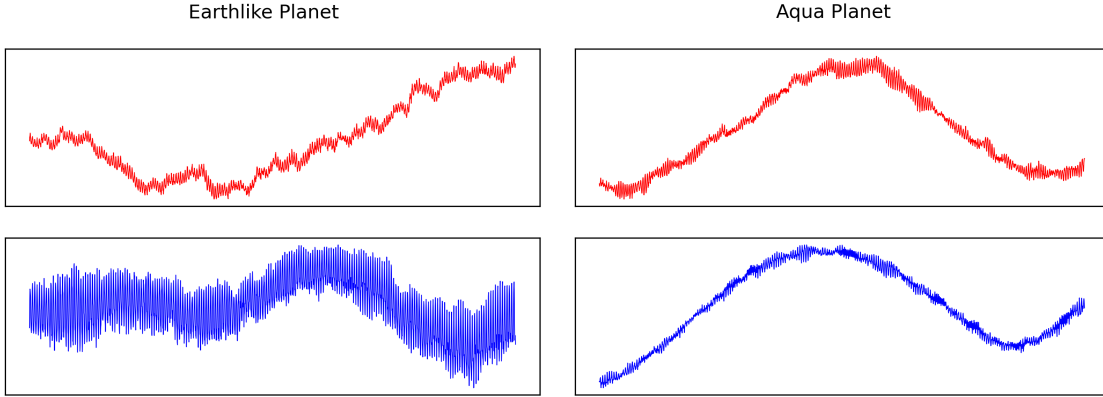


**Figure 9.** Longwave upward flux (in red) and shortwave upward flux (in blue) for Earth-like and Aqua planets.

The difference is most likely influenced by the vegetation on the Earth-like planet. To find if there is a correlation between plant coverage and reflected radiation, the longwave upward flux time-series is compared with normalized difference vegetation index time-series from 02/01/2000 to 12/31/2015.

Healthy vegetation reflects less visible light but more infrared light compared to unhealthy vegetation. Using this difference, the normalized difference vegetation index is calculated according to

$$NDVI = \frac{(IR-VIS)}{(IR+VIS)}. \quad (1)$$

Where  $IR$  is the infrared irradiance and  $VIS$  is the visible irradiance. An NDVI value closer to 1 represents healthy vegetation.

To fit the NDVI data to the longwave upward flux, the values for the same months over 15 years are averaged and scaled to fit in the longwave graph. As seen in Figure 10, there is a correlation between reflected infrared radiation and vegetation cover. The correlation becomes even more pronounced if the simulation does not have clouds.

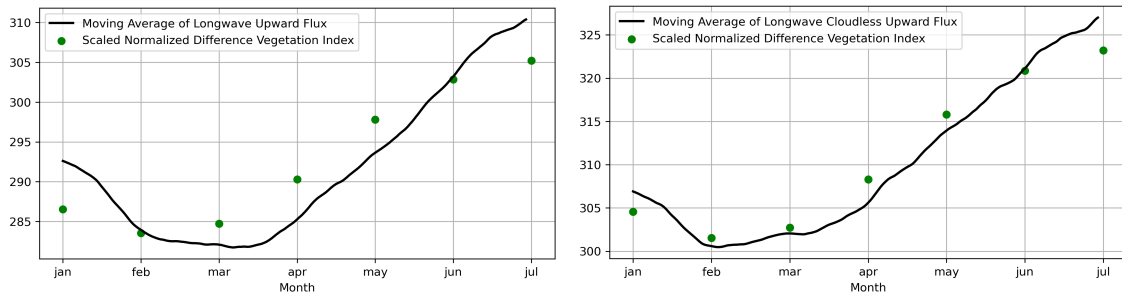


**Figure 10.** Moving average of longwave upward flux (left panel) and the moving average of longwave cloudless upward flux (right panel) compared with the scaled normalized difference vegetation index.

In future observations of exoplanets, shortwave upward flux and longwave upward flux data could be used to determine the planet's surface composition. For example, in cases where the absorption of visible light or ultraviolet radiation is greater than that of infrared light, the surface of such planet most likely consists of materials that absorb light of specific wavelengths, such as gold, copper, and silver as seen in Figure 15 (Goncalves. 2020). Furthermore, when the

trend of the time-series for shortwave upward flux is the opposite of that of longwave upward flux, the exoplanet could have vegetation similar to those on Earth.

## 7. Summary & Future Research

In this research, Fourier transform is used as a focus to determine an exoplanet's rotational period from single-pixel observations. Methodologies such as detrending and compiling different sampling intervals are applied to test whether the correct rotational period could be taken from long sampling intervals. The result for the compiling method is a discernible rotational period using sampling intervals with more than twice its length, compared to a singular Fourier power spectrum that shows the correct period with two or more daily samples.

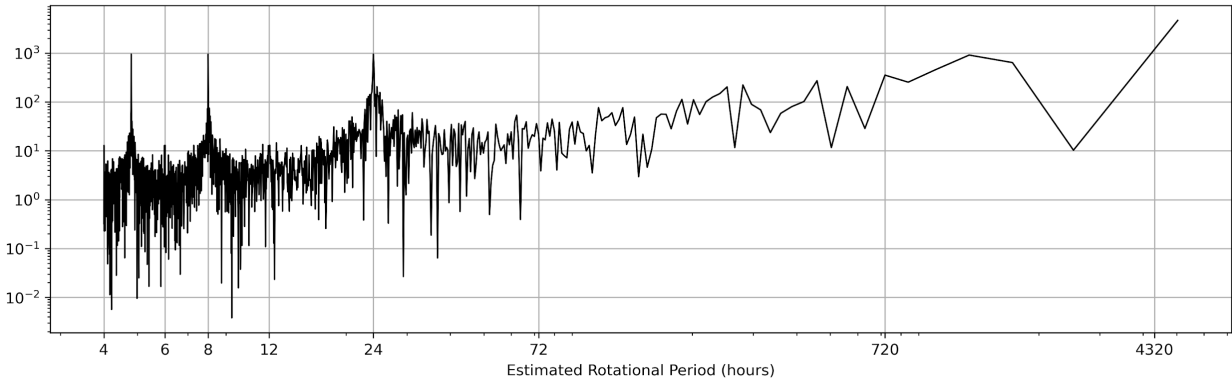
Outside of the main objective of this research, analysis is also performed on different irradiance wavelengths. By comparing the shortwave upward flux and longwave upward flux of a planet, we could find out the possible material composition on its surface, or vegetation that performs photosynthesis.

Future research still needs to be conducted on several points in this research. For one, the effect that the imaginary component has on Fourier power spectra and whether to include the imaginary number axis to the spectra. Additionally, reflectance spectra for different materials need to be studied so that the comparison between shortwave and longwave upward flux could yield better predictions of a planet's surface material.

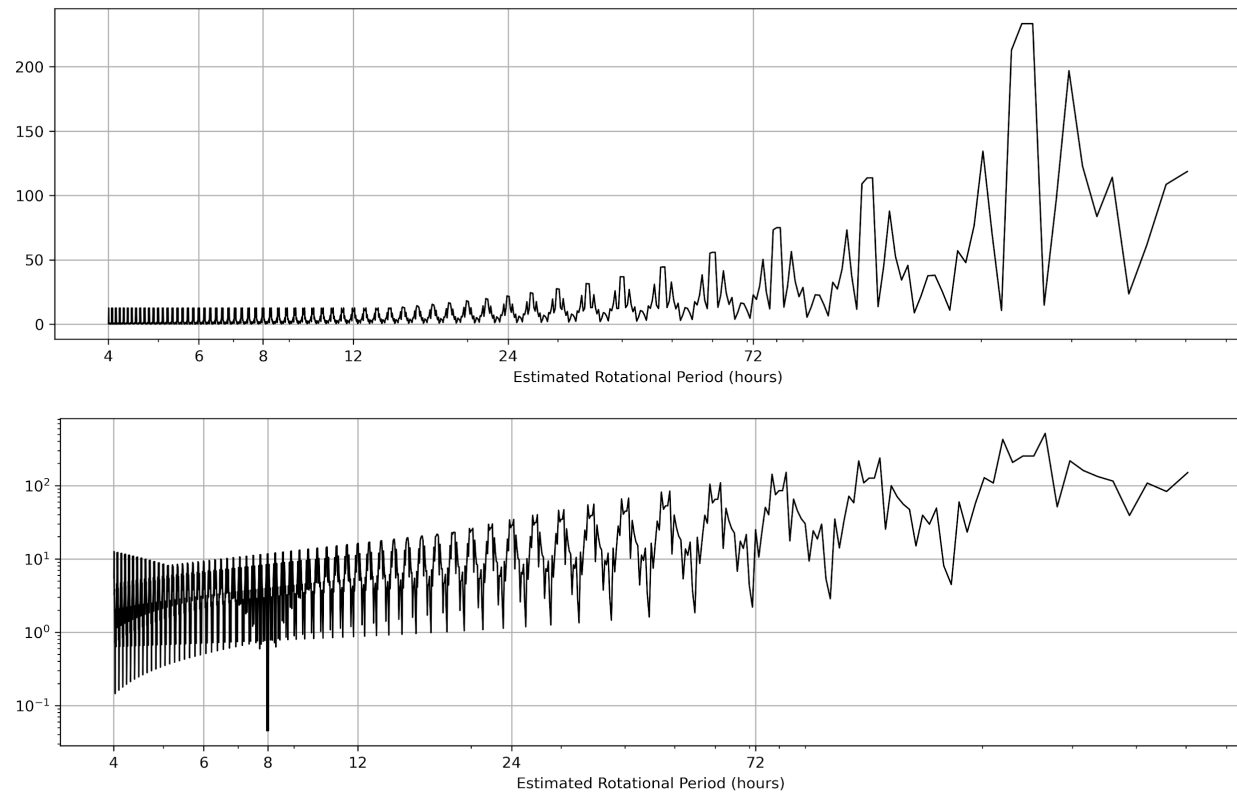
*Data and code availability:* The Simulated exoplanet data used for this study is provided by the University of Chicago group. The computer code used during the study is available publicly at <https://github.com/William-Cen/Simulated-Earth-Spectral-Analysis>.

## Appendix

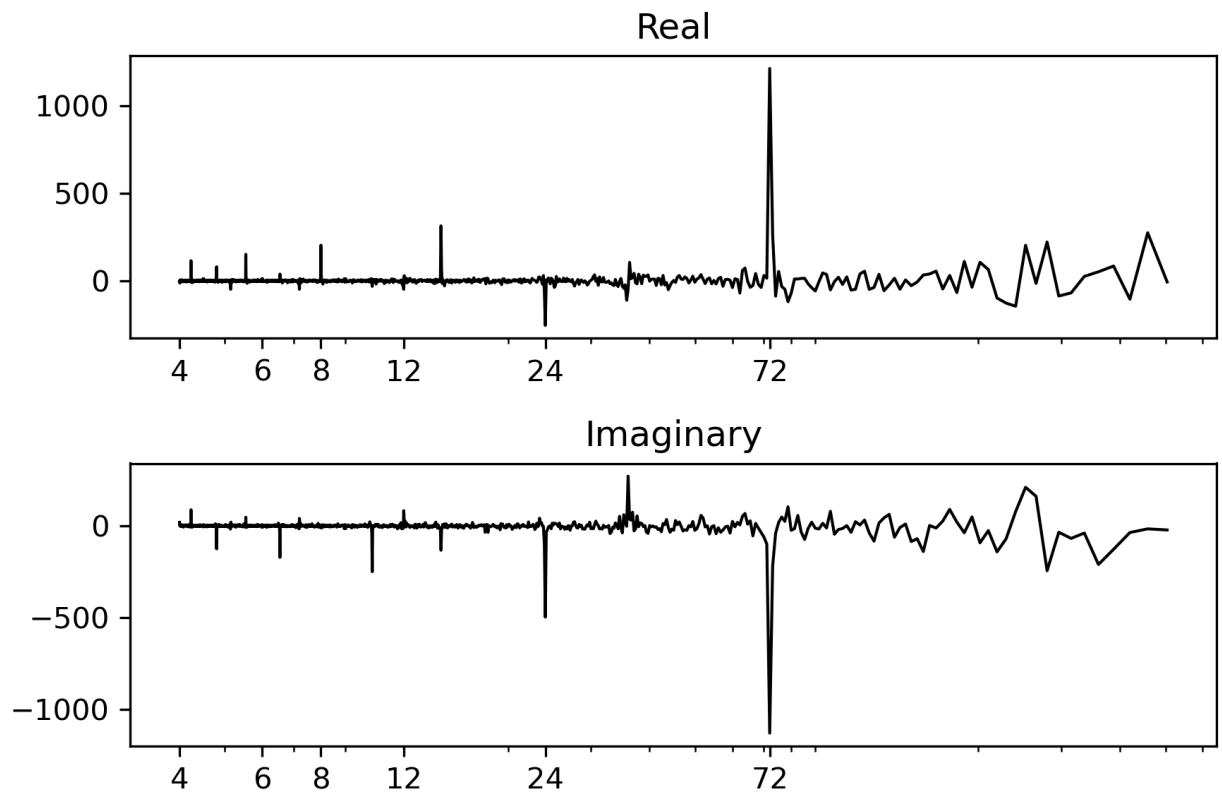
This appendix includes additional figures that are referenced in the main text.



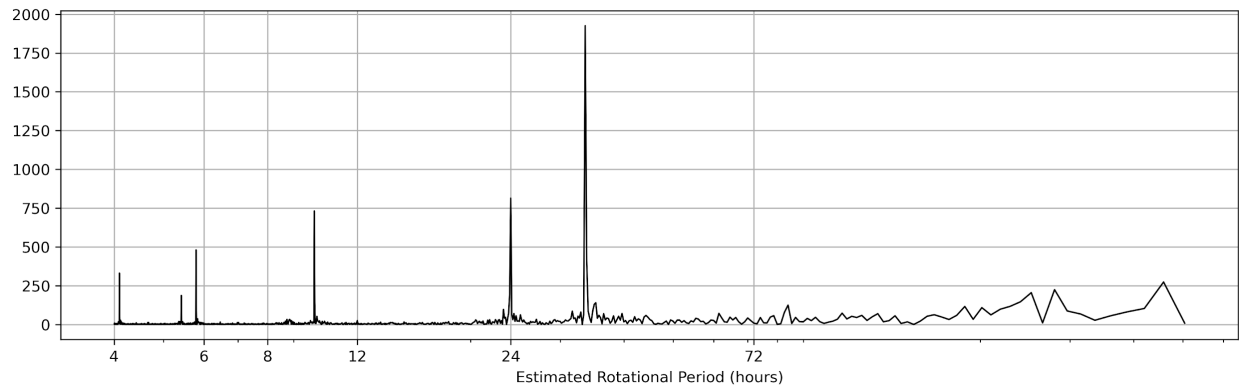
**Figure 11.** Fourier power spectrum of the Earth-like planet with a sampling interval of 12 hours (shortwave upward flux).

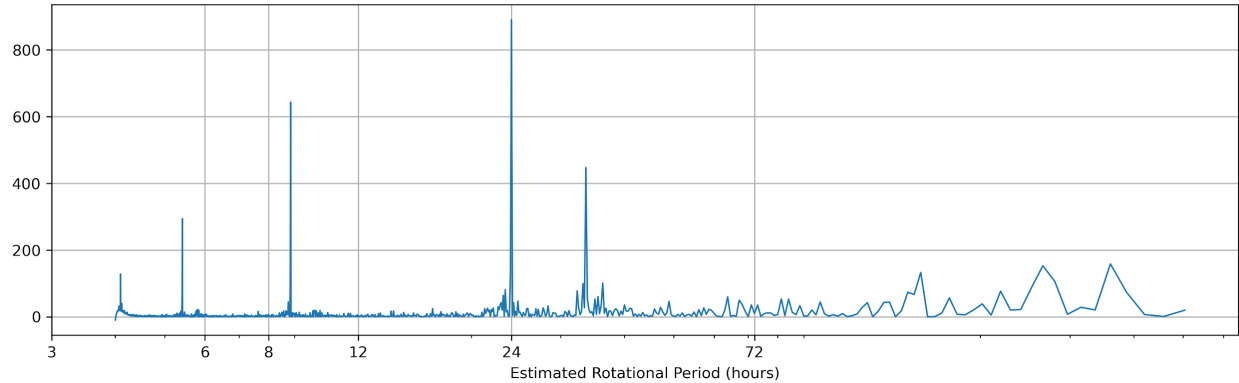


**Figure 12.** Fourier power spectrum of the Earth-like planet with a sampling interval of 240 hours (shortwave upward flux).

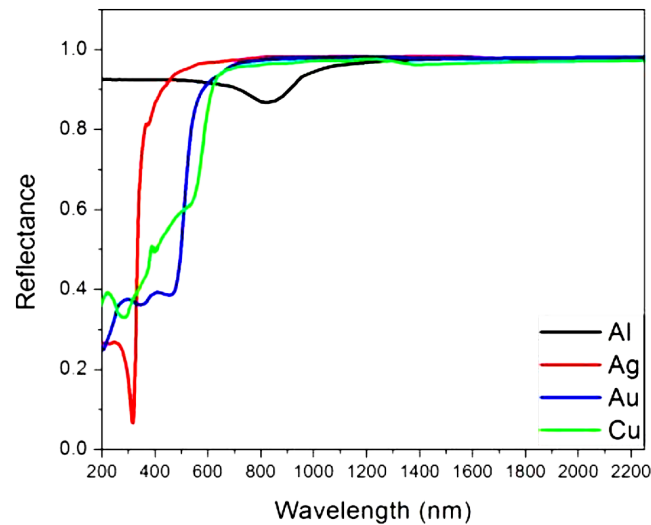


**Figure 13.** Fourier power spectrum of the Earth-like planet with a sampling interval of 18 hours (shortwave upward flux). The top panel shows the real number component from the Fourier transform and the bottom panel shows the imaginary component.

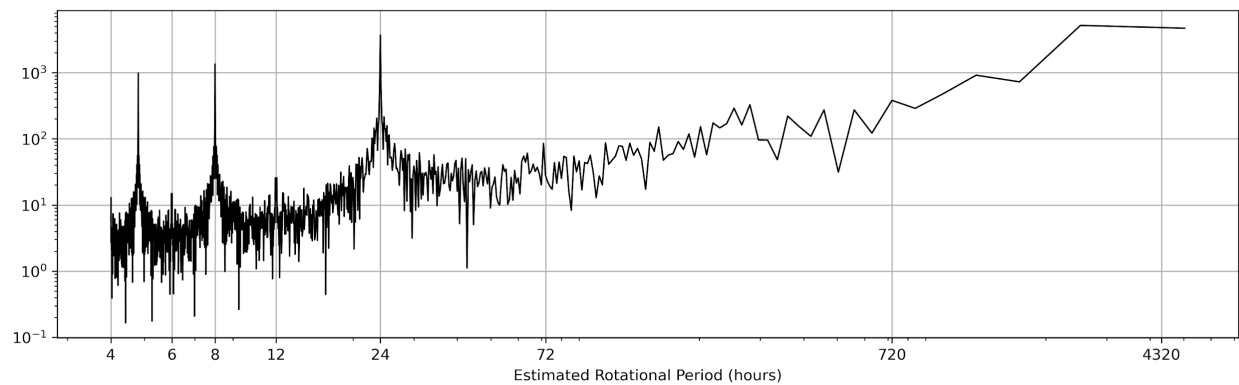




**Figure 14.** Fourier power spectrum of the Earth-like planet with a sampling interval of 14 hours (top panel), and its detrended graph using a 50th order polynomial (shortwave upward flux).



**Figure 15.** Reflectance spectra of the metals: aluminum (black), silver (red), gold (blue) and copper (green).



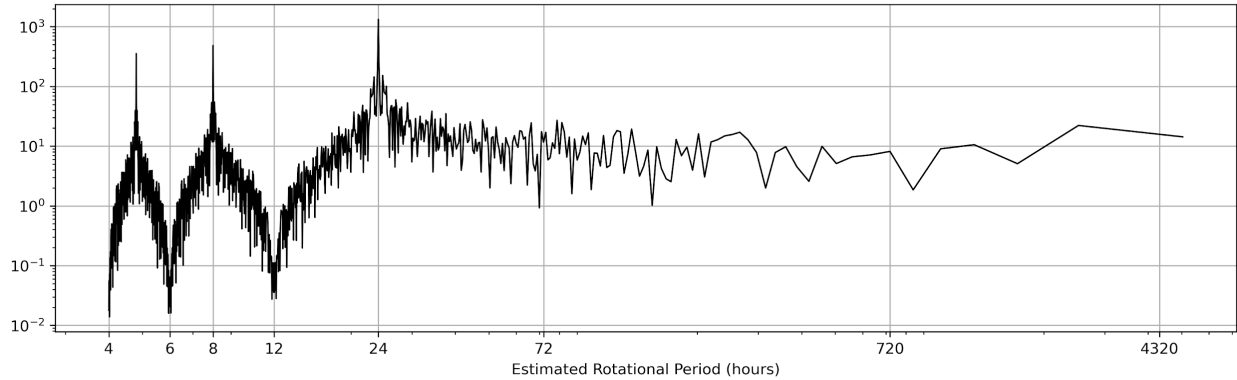


**Figure 16.** Fourier power spectrum of the Earth-like planet with a sampling interval of 12 hours (shortwave upward flux). The top panel shows Fourier transform applied to the original dataset, and the bottom panel shows Fourier transform applied to the 1st discrete difference along the dataset.

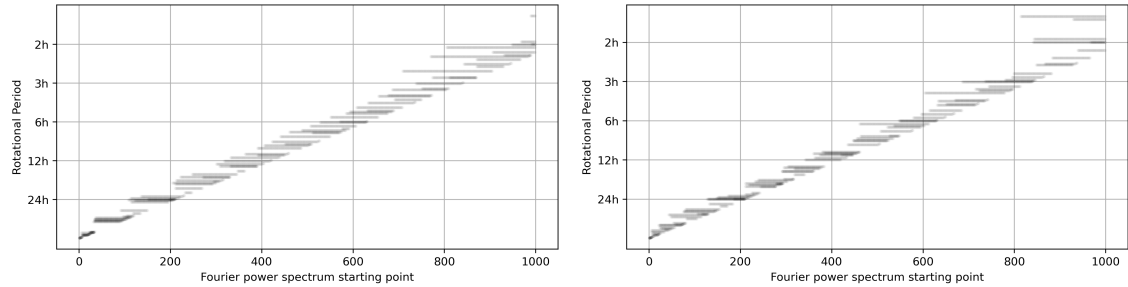


**Figure 17.** Compiled graphs for a sampling interval of 42 hours to 54 hours with the most likely rotational periods at different Fourier power spectrum starting points (left panel), and the compiled graphs of sampling intervals from 60 hours to 72 hours (right panel).

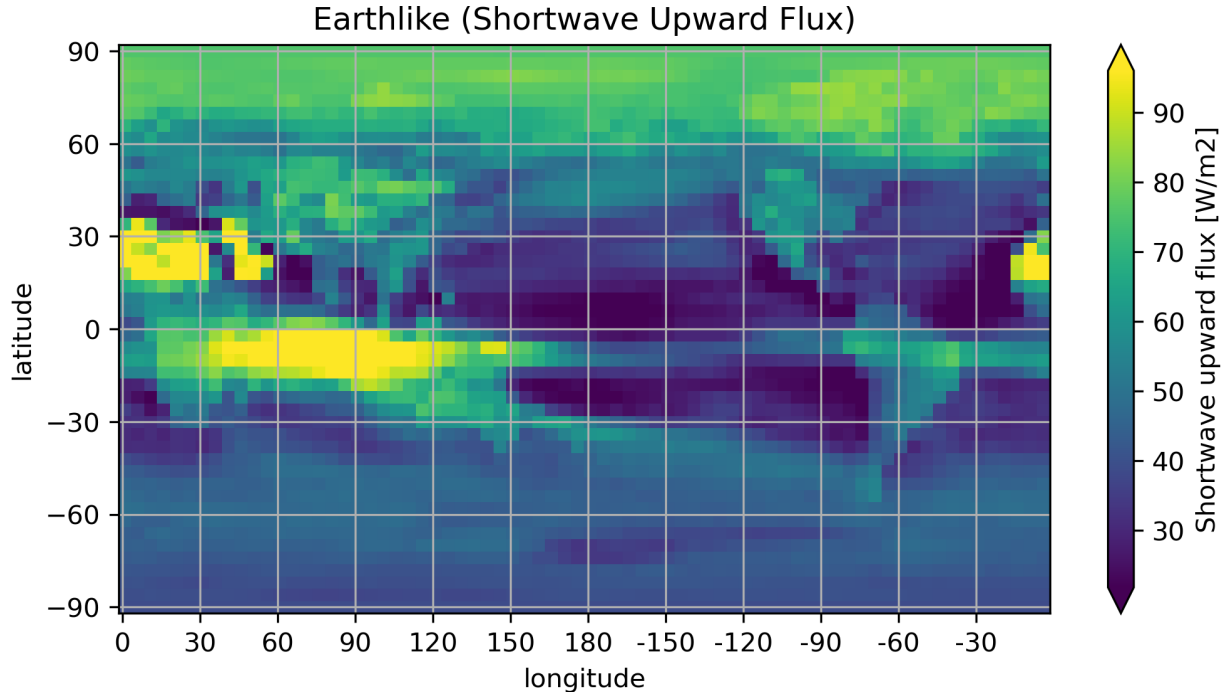


**Figure 18.** Averaged shortwave upward flux from January to July.

## References

- Jiang, J. H., Zhai, A. J., Herman, J., Zhai, C., Hu, R., Su, H., Natraj, V., Li, J., Xu, F., & Yung, Y. L. (2018). Using deep space climate observatory measurements to study the earth as an exoplanet. *The Astronomical Journal*, 156(1), 26. <https://doi.org/10.3847/1538-3881/aac6e2>
- Goncalves, A. D. (2020, May 18). *Metallic Reflection*. LibreTexts. [https://eng.libretexts.org/Bookshelves/Materials\\_Science/Supplemental\\_Modules\\_\(Materials\\_Science\)/Optical\\_Properties/Metallic\\_Reflection](https://eng.libretexts.org/Bookshelves/Materials_Science/Supplemental_Modules_(Materials_Science)/Optical_Properties/Metallic_Reflection)
- GES DISC Northern Eurasian Earth Science Partnership Initiative Project (2006), MODIS/Terra Monthly Vegetation Indices Global 1x1 degree V005, Greenbelt, MD, USA, Goddard Earth Sciences Data and Information Services Center (GES DISC), Accessed: [07/04/2020], [https://disc.gsfc.nasa.gov/datacollection/MODVI\\_005.html](https://disc.gsfc.nasa.gov/datacollection/MODVI_005.html)